



This is a repository copy of *In Candida albicans phosphorylation of Exo84 by Cdk1-Hgc1 is necessary for efficient hyphal extension.*

White Rose Research Online URL for this paper:
<http://eprints.whiterose.ac.uk/77976/>

Article:

Caballero-Lima, D. and Sudbery, P.E. (2014) In *Candida albicans* phosphorylation of Exo84 by Cdk1-Hgc1 is necessary for efficient hyphal extension. *Molecular Biology of the Cell*.

<https://doi.org/10.1091/mbc.E13-11-0688>

Reuse

Unless indicated otherwise, fulltext items are protected by copyright with all rights reserved. The copyright exception in section 29 of the Copyright, Designs and Patents Act 1988 allows the making of a single copy solely for the purpose of non-commercial research or private study within the limits of fair dealing. The publisher or other rights-holder may allow further reproduction and re-use of this version - refer to the White Rose Research Online record for this item. Where records identify the publisher as the copyright holder, users can verify any specific terms of use on the publisher's website.

Takedown

If you consider content in White Rose Research Online to be in breach of UK law, please notify us by emailing eprints@whiterose.ac.uk including the URL of the record and the reason for the withdrawal request.



eprints@whiterose.ac.uk
<https://eprints.whiterose.ac.uk/>

In *Candida albicans* phosphorylation of Exo84 by Cdk1-Hgc1 is necessary for efficient hyphal extension.

David Caballero-Lima and Peter E. Sudbery*

* Corresponding author

Department of Molecular Biology and Biotechnology

University of Sheffield

Western Bank

Sheffield S10 2TN

UK

Email: P.Sudbery@shef.ac.uk

Tel: +44 (0)1142226186

Fax: +44 (0)114 2222800

Running title: Exo84 phosphorylation by Cdk1

Key words: Exocyst/cylin dependent kinase/ Hgc1/hyphae

Abstract

The exocyst, a conserved multiprotein complex, tethers secretory vesicles before fusion with the plasma membrane; thus it is essential for cell surface expansion. In both *Saccharomyces cerevisiae* and mammalian cells cell surface expansion is halted during mitosis. In *S. cerevisiae* phosphorylation of the exocyst component Exo84 by Cdk1-Clb2 during mitosis causes the exocyst to disassemble. Here we show that the hyphae of the human fungal pathogen *Candida albicans* continue extending throughout the whole of mitosis. We show that CaExo84 is phosphorylated by Cdk1, which is necessary for efficient hyphal extension. This action of Cdk1 depends on the hyphal-specific cydin Hgc1, the homologue of G1 cyclins in budding yeast. Phosphorylation of CaExo84 does not alter its localization, but alters its affinity for phosphatidylserine allowing it to recycle at the plasmamembrane. The different action of Cdk1 on CaExo84 and ScExo84 is consistent with the different locations of the Cdk1 target sites in the two proteins. Thus, this conserved component of polarised growth has evolved so that its phospho-regulation mediates the dramatically different patterns of growth shown by these two organisms.

Introduction

Candida albicans can grow in budding yeast, pseudohyphal and true hyphal forms (Sudbery *et al.*, 2004). This morphological plasticity is essential for virulence of this major human fungal pathogen. In the hyphal state growth is highly polarised to the tip (Soll *et al.*, 1985). Such polarised growth requires a constant supply of secretory vesicles that fuse with the plasma membrane at the tip (Caballero-Lima *et al.*, 2013; Sudbery, 2011). These vesicles are necessary for cell surface expansion as they supply the additional membrane necessary for expansion of the plasma membrane. Vesicles also deliver the means to synthesise new cell wall such as integral membrane glucan synthases that manufacture β , 1,3 glucan and β 1,6 glucan, chitin synthases, cell wall remodelling enzymes, and the

mannosylated proteins that form the outer layer of the cell wall (Kis *et al.*, 2006). Studies in the model yeast *Saccharomyces cerevisiae* have shown that before fusion secretory vesicles must be tethered to the plasma membrane by an evolutionary conserved, multiprotein complex called the exocyst. This complex consists of eight subunits, Sec3, Sec5, Sec6, Sec8, Sec10, Sec15, Exo70 and Exo84 (Brennwald and Rossi, 2007; He and Guo, 2009; Heider and Munson, 2012; Terbush *et al.*, 1996; Terbush and Novick, 1995). In *S. cerevisiae* these proteins localise to sites of polarised growth such as small buds and the site of septum formation. Sec3, and part of the Exo70 pool, is thought to localize independently of the cytoskeleton (Boyd *et al.*, 2004; Finger *et al.*, 1998). Exo70 is an effector of and interacts with the Rho-type GTPases, Rho3 and Cdc42 while Sec3 interacts with Rho1 (Adamo *et al.*, 1999; Guo *et al.*, 2001; He *et al.*, 2007b; Roumanie *et al.*, 2005; Wu *et al.*, 2010; Zhang *et al.*, 2001). Both Exo70 and Sec3 interact with phosphoinositol 4,5 phosphate (PI(4,5)P₂) (He *et al.*, 2007a; Zhang *et al.*, 2008). The Remaining Exocyst components are thought to arrive on incoming vesicles (Boyd *et al.*, 2004).

In *C. albicans* exocyst subunits localise to a surface crescent at the hyphal tip (Jones and Sudbery, 2010). In contrast, vesicle-associated proteins such as Sec4, Sec2, and Mlc1 localize to a subapical spot that is clearly distinct from the surface crescent of the exocyst and is reminiscent of the Spitzenkörper long known to drive the polarised growth of other filamentous fungi (Bishop *et al.*, 2010; Crampin *et al.*, 2005; Jones and Sudbery, 2010). These different localisation patterns suggest that at least during the polarised growth of hyphae, the exocyst is already present on the plasma membrane to tether the vesicles as they arrive. Such a notion is supported by FRAP and FLIP experiments that show that the Sec2, Sec4 and Mlc1 are much more dynamic than exocyst components. Furthermore, disruption of the actin cytoskeleton leads to the immediate dispersal of Sec4 from the Spitzenkörper, while exocyst components disperse more slowly from the surface crescent. (Jones and Sudbery, 2010)

As well as controlling progress through the cell cycle, it is becoming increasingly apparent that the cyclin dependent kinase, Cdk1 (Cdc28), controls cell growth in *S. cerevisiae* (Goranov and Amon, 2010; McCusker *et al.*, 2007). In *C. albicans* the cyclin Hgc1 is specifically induced during hyphal growth and is necessary for normal hyphal morphology and growth (Zheng *et al.*, 2004). Hgc1 is the homolog of the Cln1/2 G1 cyclin pair of *S. cerevisiae*. Cells lacking Hgc1 are unable to maintain hyphal growth. When induced to form hyphae such cells evaginate a normal germ tube but this quickly swells, especially after the formation of the first septin ring. A number of targets for Cdk1-Hgc1 have been elucidated such as the Cdc42 GAP Rga2, Sec2, the septin Cdc11 and the transcription factor Efg1 (Bishop *et al.*, 2010; Snha *et al.*, 2007; Wang *et al.*, 2009; Zheng *et al.*, 2007). G2 cyclins in *C. albicans* are represented by Cb2, the ortholog of *S. cerevisiae* Cb2, and Cb4 the ortholog of *S. cerevisiae* Cb4. Cb2 is essential, depletion of Cb2 using the *MET3* regulated promoter results in cell cycle arrest with highly elongated buds, while Δ Cb4 cells are viable but show constitutive pseudohyphal growth (Bensen *et al.*, 2005).

In *S. cerevisiae* it has recently been shown that phosphorylation of the exocyst subunit Exo84 by Cdk1 – Cb2 causes cell growth to cease just before the metaphase to anaphase transition (Luo *et al.*, 2013). Exo84 plays a key role in the assembly of the exocyst. Its phosphorylation by Cdk1-Cb2 causes the exocyst complex to disassemble blocking exocytosis and cell surface expansion. Both *Sc*Exo84 and *Ca*Exo84 show a similar domain organisation consisting of a coil-coiled Vps51 domain that in Vps51 is required for the formation of the VFT docking complex mediating the fusion of late endosomes with the Golgi (Sniosoglou and Pelham, 2002), a central Pleckstrin homology (PH) domain and a C-terminal rod-like domain composed of multiple α -helices that is responsible for the interaction with other members of the exocyst complex (Fig. 1A). Luo *et al.* studied the effects of Cb2-Cdk1 phosphorylation of *Sc*Exo84 at two full Cdk1 consensus target sites (S/T.P.X.R/K) and three minimal target sites (S/T.P). In view of the observation that phosphorylation of *Sc*Exo84 disrupts interaction with other exocyst subunits, it is significant that one of the full consensus sites in

ScExo84 is located within the C-terminal interaction domain (S716). Interestingly, there is no corresponding site in the C-terminal domain of CaExo84 (Fig. 1A,B). However, CaExo84 contains a full site within the PH domain (S384) which is absent in ScExo84 (Fig. 1A,B). Two more full sites are located in CaExo84 at S256 and T488 which a Clustal alignment suggests may correspond to S291 and T496 respectively in ScExo84 (Fig. 1B). Modelling of CaExo84 shows that these sites are located either side of the PH domain in the folded protein (Fig. 1A).

Although cessation of cell growth during mitosis is a common feature among eukaryote cells, we show here that *C. albicans* hyphae continue growing throughout mitosis and cytokinesis. Moreover, the localisation of both the Spitzenkörper and the exocyst is unaltered throughout mitosis. However, we show that CaExo84 is phosphorylated by CaCdk1 in a hyphal-specific fashion, and that this phosphorylation is dependent on the hyphal specific Hgc1 cyclin rather than a G2 cyclin. Moreover, in direct contrast to budding yeast, this phosphorylation of Exo84 is essential for the rapid polarised growth of hyphae and normal hyphal morphology. Our study suggests that a role of the phosphorylation is to dissociate Exo84 from the plasma membrane by lowering its affinity for phosphotidylserine.

Results

***C. albicans* hyphae continue growing throughout mitosis and cytokinetic ring contraction**

In order to investigate whether *C. albicans* hyphae continue to extend throughout mitosis we constructed strains in which the nucleolar protein Nop1 was fused to YFP to track the nucleus, in addition, either Mlc1 or Exo70 were also fused to YFP. Initially, we followed hyphal growth throughout two complete cell cycles in the strain expressing Nop1-YFP and Mlc1-YFP after hyphae were induced from stationary phase, unbudded yeast cells. We recorded images at 60s intervals (movie 1). As visualised by Nop1-YFP the nucleus migrates out of the mother cell and divides within the germ tube as reported previously (Sudbery, 2001). This is followed 20 minutes after anaphase by contraction of the cytokinetic ring visualised by Mlc1-YFP. A second anaphase occurred after 30 minutes which in turn was followed by cytokinetic ring contraction 20 minutes later. Throughout the whole of these two cycles the hyphae extended at a constant rate of $0.33\mu\text{m min}^{-1}$ (Fig. S1A). Close examination around the time of the two mitoses and the two contractions of the cytokinetic ring showed that hypha growth continued to extend during these events at a rate consistent with the long term average rate of hyphal extension (Figs. S1 B,C).

It may be argued that the cessation of growth occurs on a shorter time scale than the 60s intervals between frames in Movie 1. We therefore investigated the growth of cells over shorter time scales. Moreover, it was of interest to visualise the Spitzenkörper, as this is a sensitive indicator of polarised growth of fungal hyphae, and the exocyst to discover if it dispersed as it does in *S. cerevisiae* during metaphase. We therefore recorded images over 10s intervals throughout mitosis for the Nop1-YFP Mlc1-YFP strain and 20s intervals for the Nop1-Exo70 strain. These experiments were complicated by the extreme sensitivity of mitosis to the excitation light; for this reason the frame rate was increased to 20s for the Nop1-YFP Exo70 YFP strain. The full movies are shown in movie 2 and movie 3 for Mlc1-YFP Nop1-YFP and Nop1-YFP Exo70-YFP respectively. Consecutive frames spanning a mitosis are shown in Fig. 2 for Mlc1-YFP Nop1-YFP and Fig. S2 for Nop1-YFP Exo70-YFP. Interestingly in the Nop1-YFP Mlc1-YFP strain a pair satellite spots appeared either side of the nucleus just before anaphase that may represent recruitment of a myosin to the Spindle Pole Body during metaphase. Evidence for a myosin role in the mitotic spindle has recently been reviewed (Sandquist *et al.*, 2011). Fig. 2A shows that growth continued throughout mitosis, so that the tip extended by $0.8\mu\text{m}$ in the 140s of the movie shown in Fig. 2A, consistent with the long term average growth rate of $0.33\mu\text{m}\cdot\text{min}^{-1}$ (Fig. S1). Using a combination of FRAP and FLIP we previously showed that vesicles enter

and leave the Spitzenkörper with a turnover time of 30s (Jones and Sudbery, 2010). The Spitzenkörper remained in place before, during and after mitosis, and the intensity of Mlc1-YFP did not diminish throughout metaphase and anaphase. This suggests that vesicle traffic into the Spitzenkörper and from the Spitzenkörper to the cell surface continued throughout mitosis. Fig. S2 shows that throughout mitosis the exocyst component Exo70 also remained as a crescent at the hyphal tip and that the hyphal tip continued to extend. Thus hyphal extension and polarised exocytosis continue throughout mitosis.

Exo84 is phosphorylated by Cdk1 in a hyphal-specific fashion

In order to investigate whether Exo84-YFP is phosphorylated, we looked for a band shift on 1D PAGE gels before and after λ phosphatase treatment using a monoclonal antibody to YFP in a Western blot experiment. Fig. 3A shows that Exo84-YFP extracted from exponentially growing yeast cells shows a small band shift, whereas Exo84 extracted from hyphae shows a larger band shift. In order to investigate in more detail the pattern of phosphorylation we fractionated Exo84-YFP using 2D gels (Fig. 2B). Stationary phase yeast cells show 4 weak spots; whereas exponentially growing yeast cells show three further spots. Thus Exo84 is phosphorylated under yeast growth conditions consistent with the small band shift we observed in 1D gels. In order to study the temporal pattern of phosphorylation in hyphal cells we analysed samples recovered 30, 60 and 90 minutes after inoculation into hyphal growth conditions. Exo84 became more phosphorylated with the spots moving progressively towards the acidic end of the pH range (Fig. 3B). By 90 minutes three of the additional spots appeared to correspond to the three spots visible in growing yeast, but they are more intense in the hyphal sample. A fourth spot is clearly unique to hyphal growth. Since this is the most acidic, it corresponds to the most highly phosphorylated form of the protein.

C. albicans Exo84 contains 3 matches to the full Cdk target motif (T/S.P.X.R/K) at positions S256, S384 and T488. Since it is known that Hgc1, the hyphal specific Cdk1 cyclin, is required for hyphal growth we examined whether the hyphal-specific band shift depended on the presence of Hgc1. Figs. 3B, and 3C shows that this is indeed the case. Exo84-YFP extracted from a $\Delta hgc1$ strain shows only a slight increase in phosphorylation compared to the stationary phase control in 2D gels (Fig. 3B). In 1D gels the band shift observed in wild type cells was absent in the $\Delta hgc1$ strain (Fig. 3C).

In *S. cerevisiae* it has been reported that Cdk1 partnered by Clb2 phosphorylates Exo84 to arrest cell growth during mitosis (Luo *et al.*, 2013). Because deletion of Clb2 is lethal in *C. albicans* we used a strain in which Clb2 was expressed from the regulatable *MET3* promoter to investigate its possible involvement (Bensen *et al.*, 2005). When yeast cells were grown with the *MET3* promoter repressed, cells arrested with an elongated phenotype as previously reported confirming that Clb2 was successfully depleted. We found that hyphae induced in the absence of Clb2 arrested after the first nuclear division, and showed no change in the Exo84 phosphorylation (Fig. 3D). Similarly, we found no change in the phosphorylation of Exo84-YFP when *CLB4* expression was repressed in a *MET3-CLB4* strain (Bensen *et al.*, 2005) (Fig. 3D). Thus, the phosphorylation of Exo84 is dependent on Cdk1 partnered by Hgc1.

To further confirm the requirement for Cdk1 we examined whether the band shift was present when a strain expressing only the analogue-sensitive Cdk1-*as1* allele was inhibited by the presence of 1NM-PP1. As shown in Fig. 3E the hyphal-specific band shift disappeared in the presence of 1NM-PP1. To investigate whether Cdk1 directly phosphorylates Exo84 we carried out an *in vitro* kinase assay with recombinant GST-Exo84 as the substrate and Cdk1 purified from *C. albicans* hyphae. To monitor the reaction we used an antibody specific to phosphorylated serine in the full motif recognised by cyclin-dependent kinases (S.P.X.R/K) (hereafter referred to as α pS-Cdk). Recombinant wild type Exo84 was phosphorylated by purified Cdk1, but recombinant GST-Exo84 in which the three Cdk target sites had been substituted by alanine (Exo84-3A) was not a substrate (Fig. 3F). To demonstrate that the active kinase was Cdk1 and not a co-purifying kinase, we repeated the

experiment using purified Cdk1-as1 carrying the analogue sensitive allele. As we experienced before (Bishop *et al.*, 2010), this kinase shows lower activity *in vitro* even in the absence of inhibitor, suggesting it is not fully active. Nevertheless it is clear that in the absence but not the presence of 1NM-PP1 Exo84 is phosphorylated *in vitro*, demonstrating that the active kinase is Cdk1 (Fig. 3G).

We used the α S-Cdk antibody to investigate the pattern of Cdk1-specific phosphorylation of Exo84 *in vivo* (Fig. 4). Exo84 extracted from wild type cells reacted strongly with this antibody from 30 minutes after hyphal induction onwards. Exo84 extracted from $\Delta hgc1$ cells showed strongly reduced phosphorylation consistent with the conclusion that Cdk1-Hgc1 is targeting Exo84. In order to confirm that the three full Cdk1 targets are involved we constructed mutants in which these sites were mutated (described in more detail below). The strain in which all of the three Cdk1 target sites were mutated to alanine (Exo84-3A) was barely viable, producing slow-growing yeast cells that were greatly enlarged and failed to show any polarised growth in response to hyphal-inducing cues. We have not characterised this strain further. The strain in which both S256 and S384 were mutated to alanine (Exo84-2A) showed significant hyphal defects as we document below. In a Western blot using the α S-Cdk antibody a, Exo84-2A showed significantly less phosphorylation than the wild type (Fig. 4). We also used 2D gels to examine the pattern of phosphorylation during hyphal growth in Exo84-2A and in two further mutants: a non-phosphorylatable alanine substitution at residue T488 (Exo84-T488A), and Exo84-3E where the three putative phospho-acceptor sites had been mutated to phosphomimetic glutamate. In these 2D gels, both in Exo84-2A and the Exo84-T488A proteins showed reduced phosphorylation consistent with these residues being the target of Cdk1-Hgc1 (Fig. 3B). However, it was not possible to associate any particular residue with the discrete spots observed in the 2D gel of wild type Exo84 extracted from hyphal-grown cells. Exo84-3E showed a shift towards the acidic end of the pH range, consistent with the increased negative charge of the glutamate residues.

Phosphorylation of Exo84 is required for the highly polarised growth of hyphae.

To investigate the physiological role of Exo84 phosphorylation we first confirmed that Exo84 is essential in *C. albicans*. In the diploid genome of *C. albicans* the upstream sequence of Exo84 is different in the two alleles. A retrotransposon of the Gypsy group is inserted 79 base pairs upstream of allele Orf19.135; whereas in allele Orf19.7779 the 3' end of *SIF2* (Orf19.7778) is located 236 bp upstream of the start of the *EXO84* ORF. Deletion of either *EXO84* ORF has no major phenotypic effect; thus both alleles are functional and haplosufficient. When the remaining allele is placed under the control of the regulatable *MAL2* promoter cells are unable to grow on glucose which represses the *MAL2* promoter (Fig S3A). Thus Exo84 is essential. Depletion of Exo84 results in round, enlarged cells with wide necks and with some cells containing multiple nuclei; suggesting that Exo84 is required for polarised growth and cytokinesis, as it is in *S. cerevisiae*, (Fig. S3B).

We constructed strains in which the only copy of Exo84 carried non-phosphorylatable alanine substitutions at each of the putative Cdk1 phosphorylation sites (Exo84-S256A, Exo84-S384A, Exo84-T488A), we combined the mutations to make double (Exo84-S256A S384A) and triple mutants (Exo84-S256A S384A T488A), hereafter called Exo84-2A and Exo84-3A respectively. We also constructed phosphomimetic substitutions at the T488 site (Exo84-T488E) and at all three putative sites (Exo84-S256E S384E T488E) hereafter called Exo84-3E. All of these strains were constructed with C-terminal YFP fusions. Fusing the remaining copy of *EXO84* in the heterozygous strain to YFP had no phenotypic consequences, thus the Exo84-YFP is a functional protein. We carried out Western blots using an α GFP antibody which confirmed that each of these proteins were present in amounts comparable to the wild type level (data not shown).

As described above the strain expressing only Exo84-3A was severely affected and we have not characterised this strain further. The Exo84-2A strain showed significant morphological abnormalities in the hyphal form compared to wild type (Fig. 5A,B). Quantitation showed that there was a

significant increase in the number of pseudohyphal cells compared to wild type (Fig. 5F) and in addition some hyphae showed a phenotype similar to the $\Delta hgc1$ phenotype, that is, a short normal appearing germ tube which quickly reverted to less polarized growth resembling pseudohyphae. We refer to these cells as “other” since they neither resemble hyphae or pseudohyphae. Although a significant proportion of Exo84-2A cells made hyphae that were morphologically normal, these hyphae were extended at approximately half the rate of wild type hyphae (Fig. 5G). Thus phosphorylation of Exo84 is necessary to allow the highly polarised growth characteristic of hyphae. The strain only expressing the *EXO84* T488A allele was similarly affected showing a marked reduction in the proportion of cells showing a normal hyphal morphology (Figs 5D-4F). Again where cells formed morphologically normal hyphae these hyphae extended at a markedly slower rate than the wild type cells (Fig. 5G). The strain carrying the *EXO84*-S384A allele also showed a reduction in the proportion of hyphal cells, and the hyphae that did form extended more slowly. However, this reduction was less extreme than the *EXO84*-2A and *EXO84* T488A strains (data not shown). The *EXO84*-S256A allele did not have a significant effect on cell morphology or hyphal extension rate (data not shown).

The fusion of Exo84 to YFP in the wild type and mutant proteins allowed us to investigate the localisation of Exo84. As we described previously, Exo84-YFP localizes to a surface crescent in wild type hyphae (Fig. 5A and inset). Exo84 is also present at the septum site during cytokinesis to promote the polarised growth necessary for the formation of secondary cell walls (Fig. 5A barbed arrows). In the Exo84-2A mutant cells Exo84-2A-YFP localized to a crescent at the tip of hyphal cells (Fig. 5B and inset). However, in cells growing in the pseudohyphal phenotype Exo84-2A-YFP relocated to the septum late in the cell cycle and was no longer present at the tip (Fig. 5B barbed arrow), consistent with our previous report that polarity components relocate from the tip of pseudohyphal cells late in the cell cycle (Crampin *et al.*, 2005). Exo84-T488A-YFP also localised to the tip of hyphal cells (Fig. 5C and inset) and, like Exo84-2A-YFP, was present at the tip or septum of pseudohyphal cells but not at both simultaneously. Figs 5C,E illustrate a phenomenon that we also occasionally observed in the Exo84-2A mutants. As can be seen in the region enlarged in Fig. 5E Exo84 becomes ectopically located with diffuse localization at the tip and an incomplete ring at the septum. Calcofluor White (CFW) staining reveals that this ectopic localization is associated with excess chitin deposition. In the yeast form both the Exo84-2A and the Exo84-T488A strains showed an increase in mother cell volume compared to wild type yeast cells (Fig. S4). However, the axial ratio (major/minor axis) was reduced showing the cells were rounder than wild type cells.

In hyphal-promoting growth conditions, cells expressing the phosphomimetic Exo84-3E allele were more similar to wild type cells than cells expressing non-phosphorylatable alleles (Fig. 5D). There was a smaller reduction in the proportion of cells that formed true hyphae (Fig. 5F) and a smaller reduction in the rate of hyphal extension (Fig. 5G). Exo84-3E yeast cells showed an increase in cell volume compared to wild type yeast cells but the axial ratio was not significantly different showing that the cell shape was not altered (Fig. S4). Interestingly, the *Exo84*-T488E allele showed a decrease in cell volume and an increased axial ratio, suggesting a longer or more pronounced phase of polarised growth during their cell cycles (Fig. S4).

While non-phosphorylatable alanine substitutions at the Cdk1 target sites impair polarised growth and hyphal morphology, phosphomimetic substitutions have only a mild effect on the hyphal phenotype. This is consistent with the hypothesis that phosphorylation of Exo84 is necessary for the extreme polarised growth of hyphae. If one of the roles of Hgc1-Cdk1 is to phosphorylate Exo84, then it is possible that the Exo-84-3E allele may alleviate some or all of the phenotypic effects of the $\Delta hgc1$ allele. To test this idea we constructed a $\Delta hgc1$ *EXO84*-3E strain. The *EXO84*-3E allele did not rescue the phenotype of the $\Delta hgc1$ allele. However, there was an increase in the proportion of hyphal cells from 1.2% to 17% (Fig. 5F). Since other functions of Hgc1-Cdc28 have been documented, it is not surprising that the *EXO84*-3E allele does not fully rescue the effects of a $\Delta hgc1$ mutation.

One such target of Hgc1-Cdk1 is Rga2, which acts as a negative regulator of hyphal growth that is relieved upon phosphorylation (Zheng *et al.*, 2007). We previously showed that while deletion of Rga2 does not induce constitutive hyphal growth, hyphal growth is initiated in $\Delta rga2$ mutants under conditions that would normally induce pseudohyphal formation (Court and Sudbery, 2007). We thus investigated whether the Exo84-3E mutant also increased the proportion hyphae when cells were grown at 35°C pH 6.0, which would normally induce pseudohyphal growth (Fig. 6.) Indeed, under these conditions the proportion of hyphae increased from 15% in wild type cells to 35% in Exo84-3E mutants. In contrast, hyphal growth was absent (Exo84-T488A) or nearly absent (Exo84-2A) in the non-phosphorylatable mutant alleles (Fig. 6). Taken together these experiments provide further support for the hypothesis that Hgc1-Cdk1 targets Exo84 at the three full consensus Cdk1 target sites to promote hyphal growth, although it is clear that Cdk1 also has other targets that must be phosphorylated for the full hyphal phenotype.

When hyphae are able to form, phosphorylation of Exo84 is not required for its localisation or exocyst assembly

Exo84 is continually present as a surface crescent at the tip of hyphae, and during cytokinesis it is simultaneously present at the site of septum formation and the hyphal tip (Figs 5A). The morphological defects resulting from the mutant alleles described above were observed in cells growing on rich YEPD medium. We found that the morphological defects of the *exo84-2A* and *exo84-T488A* alleles were less pronounced on minimal medium, so that a higher proportion had a hyphal morphology (Fig 7A). Nevertheless, these hyphae extended at a slower rate than wild type hyphae showing that the non-phosphorylatable alleles still reduced polarised growth. We took advantage of this observation to investigate whether the mutations affected the location of Exo84 to sites of septum formation during hyphal growth. We followed Exo84-YFP localisation over time in wild type and strains carrying each of the non-phosphorylatable and phosphomimetic alleles fused to YFP. Fig. 7B shows the percentage of cells displaying Exo84 in the septum plotted against time after hyphal induction. In wild type cells a peak of septum-located Exo84 occurs at 115 minutes. Cumulatively, Exo84 has been observed at the septum in 70% of wild type hyphae by 150 minutes (Figure 7C). Mutant cells that formed hyphae also showed localisation of Exo84 to the septum (Fig. 7A). However, it is observed at a later time in the septum compared to wild type cells, and the cumulative proportion of cells that have displayed septum-located Exo84 is much lower in each of the mutants (Fig. 7C). However, when Exo84 is present at the septum the total length of the hypha and the distance from the bud neck to the septum is similar in the wild type and mutants (Fig. 7D). This suggests that the delay in Exo84 location to the septum reflects an increased time to reach a critical hyphal length at which cytokinesis is initiated due to the lower extension rate of the hyphae. Thus, in these hyphal cells the presence or absence of phosphorylation does not affect Exo84 localization, but does affect the rate of polarised growth.

In *S cerevisiae* phosphorylation of Exo84 is reported to disrupt the assembly of the exocyst complex (Luo *et al.*, 2013). We showed above (Fig. S2) that Exo70 remains at the bud tip throughout mitosis. To further investigate the effect of Exo84 phosphorylation on exocyst interactions we examined whether phosphorylation of Exo84 affected its interaction with Sec10, as this interaction is disrupted in *S cerevisiae* by Exo84 phosphorylation. We constructed Exo84-GFP Sec10-HA strains in which Exo84 was wild type or carried respectively the Exo84-T488A, Exo84-2A, and 3E mutations. Using these strains we carried out reciprocal immunoprecipitation experiments. In each case the mutations did not affect the interaction of Exo84 and Sec10 (Fig. 8A,B).

Phosphorylation of Exo84 may affect phospholipid binding

Exo84 contains a pleckstrin homology (PH) domain that promotes interactions between proteins and phospholipids (Fig 1A). The S384 site is located within this domain, while protein threading suggests that the important S256 and T488 sites are either side of this domain in the folded protein (Figs 1A).

We therefore investigated if Exo84 binds phospholipids, and if so whether phosphorylation Exo84 affected the binding. To do this we used a PIP strip and recombinant GST-Exo84 and GST-Exo84-3E (Fig. 9A). Wild type GST-Exo84 appeared to have the greatest affinity for phosphatidylserine (PS) with a much weaker affinity for phosphatidic acid (PA) (Fig. 9A,B). Since this protein was expressed in *E coli* it is not phosphorylated, so this reports the affinity of the non-phosphorylated form of the protein. Interestingly, the GST-Exo84-3E protein appeared to have a considerably reduced affinity for PS consistent with the negative charge on PS and the increased negative charge on Exo84 resulting from the phosphorylation (Fig. 9A,B) Note that 8µg of recombinant Exo84-3E but only 2µg of recombinant Exo84 were loaded onto each spot in the PIP strip, thus the reduced affinity of Exo84 for PS is likely to be considerably greater than the 2.5 fold reduction shown in figure 9A.

PS is synthesised from cytidyldiphosphate-diacylglycerol (CDP-DAG) and serine by the action of phosphatidylserine synthase encoded by the *CHO1* gene (Chen *et al.*, 2010). In *C albicans* $\Delta cho1$ mutants are viable but have cell wall defects and fail to show filamentous growth on Spider medium. In addition, they are auxotrophic for ethanolamine, as phosphatidylethanolamine is synthesised from PS. To investigate further whether PS plays a role in Exo84 localization we constructed a $\Delta cho1$ Exo84-YFP strain and investigated its phenotype. We used defined medium supplemented with phosphatidylethanolamine since we found that YPD contained sufficient PS to supplement the PS auxotrophy. On defined medium this strain grew slowly. In both wild type and $\Delta cho1$ yeast cells Exo84-YFP localised to the septum and the tip of small buds (Figs. 7A,9C). However, it also showed ectopic punctate localisation to other regions of the cell periphery in $\Delta cho1$ cells (Fig. 9C). During hyphal growth, $\Delta cho1$ cells (induced on Lee's medium (Lee *et al.*, 1975)) Exo84 also showed a disturbed pattern of localisation, so that although it was present at the tip, it was also present in ectopic sites in the mother cell and within the germ tube (Fig. 9C). As a control we also constructed a $\Delta cho1$ strain expressing Sec3-YFP, which during both yeast and hyphae growth did not show the ectopic localization. (Fig. 9C). Thus the ectopic localization of Exo84 in the absence of PS is specific to Exo84 is not caused by a general failure of exocyst localisation.

While these observations suggest a role for PS in the localisation of Exo84, the role of this phosphorylation is not straightforward because phosphorylation lowers the affinity of Exo84 for PS. It may be that the phosphorylation is important to dissociate Exo84 from membranes to allow it to be recycled to the growing tip in a fashion reminiscent of recent models of the role of endocytosis in restricting localisation of Cdc42 to sites of polarised growth. To address this possibility we examined the recycling kinetics of Exo84-2A and Exo84-3E using FRAP. To avoid the application of extensive bleaching corrections during post-bleach imaging, we employed an experimental design we developed previously where we measured the fraction of fluorescence recovered in 30s (Jones and Sudbery, 2010). Exo84-2A-YFP recovered only 35% of the pre-bleach fluorescence in 30s, whereas wild type Exo84-YFP recovered 53%, a difference that was statistically significant (Fig. 10). Exo84-3E recovered 60% of pre-bleach fluorescence. Although this was more than the wild type protein, the difference was not significant. Thus, phosphorylation of Exo84 is necessary for the rapid exchange of Exo84 at the cell surface, consistent with the idea that phosphorylation promotes Exo84 recycling by promoting its dissociation from PS.

Discussion

During the growth of a bud in *S cerevisiae* or the yeast phase of *C albicans*, growth is polarised for a short period as the bud emerges, but later becomes isotropic around the whole of the bud perimeter. The period of polarised growth relative to isotropic growth must be relatively short because, as we record here, the axial ratio of the prolate spheroid *C albicans* cells is 1.5. During cytokinesis, polarised growth relocates to the site of septum formation. However, it has recently been shown in *S cerevisiae* that the fusion of secretory vesicles is blocked during metaphase and cell

surface expansion ceases (Luo *et al.*, 2013). *C. albicans* hyphae show a radically different pattern of growth compared to the yeast phase. Polarised growth is focussed to a narrow area at the hyphal tip and is continuous throughout the whole cell cycle. It does not show the polarised to isotropic switch, and we show here it does not cease at any point during mitosis or cytokinesis. Despite this radically different growth pattern, so far studies on the mechanism of polarised growth in *C. albicans* suggest that the same components are utilised as have been elaborated in the *S. cerevisiae* budding yeast model (for a review see (Sudbery, 2011). Clearly, however the machinery must be modified to produce the radically different outcome of hyphal growth.

Here we have uncovered one of the key differences. In *C. albicans* the exocyst component Exo84 is phosphorylated by Cdk1 as it is in *S. cerevisiae*. However, instead of causing the disassembly of the exocyst complex and halting the fusion of secretory vesicles necessary for cell surface expansion, phosphorylation of Exo84 in *C. albicans* is necessary for the efficient polarised growth of hyphae. Substitutions of non-phosphorylatable residues at the consensus Cdk1 phosphorylation sites causes morphological abnormalities in many cells growing on rich medium and reduces hyphal extension rates on all media. The morphological abnormalities include an increased proportion of cells that grow as pseudohyphae, as well as cells that resemble the $\Delta hgc1$ phenotype, where cells evaginate germ tubes that appear normal, but quickly revert to the less polarised growth typical of pseudohyphae. These abnormalities are not shown by cells carrying phosphomimetic substitutions at the same sites. In particular, whereas the Exo84-3A mutant is severely affected and in many ways resembles the phenotype of cells depleted of Exo84, the Exo84-3E strain shows only minor abnormalities.

We also observed that Exo84 is phosphorylated during yeast phase growth, although this was not as extensive as hyphal growth. Exo84 phosphorylation is clearly important for yeast growth as shown by the major effect of the Exo84-3A allele in the yeast phase phenotype; moreover, the mother cells of Exo84-3A, Exo84-2A and Exo84-T488A strains were rounder than the wild type. This suggests that Exo84 phosphorylation is required for the initial polarised growth of small yeast buds. Intriguingly, it has previously been reported that *S. cerevisiae* cells arrested at Start by *cdc28-4* and *cdc7-1* alleles at 37°C show increased affinity of Exo84 for other components of the exocyst (Luo *et al.*, 2013). In addition, Exo84 shows a weak reaction to the antibody recognising phosphorylated Cdk1 target sites in cells arrested at start by α -factor. Such cells form mating projections which have many similarities to hyphae (Chapa Ylazo *et al.*, 2011). Finally, the Cln2-Cdk1 kinase phosphorylates recombinant Exo84 *in vitro* (Luo *et al.*, 2013). Taken together, these observations suggest that phosphorylation of Exo84 may also play a role in polarised growth in *S. cerevisiae*.

What is the role of Exo84 phosphorylation? One of the Cdk sites is within the PH domain while the other two sites are located either side of the PH domain in the 3-dimensional model of the protein reconstructed by threading analysis (Fig. 1A). PH domains bind phospholipids in membranes, and we show here that recombinant GST-Exo84, which is not phosphorylated, has an affinity for phosphatidylserine (PS), and that this is reduced in the Exo84-3E which mimics a fully phosphorylated protein. Thus phosphorylation may regulate the affinity of Exo84 for this phospholipid. A precedent of the role of PS in polarised growth is the demonstration that in *S. cerevisiae* it is localised to sites of polarised growth and facilitates the recruitment of Cdc42-GTP to these sites. We showed that $\Delta cho1$ cells, which are unable to synthesise PS, Exo84 localised ectopically to punctate patches at the cell surface in both yeast and hyphae. Nevertheless, in these cells Exo84 also localises to sites of polarised growth such as the tip of small buds and the septum in yeast and the hyphal tip and septum in hyphae. Thus loss of PS lowers the efficiency, but does not completely prevent Exo84 localization. In *S. cerevisiae* Sec3 is thought to provide a landmark for exocyst assembly. In *C. albicans* $\Delta Sec3$ cells fail to maintain polarised growth after the formation of the first septum, a phenotype that depends on the presence of Cdc11 in the septin ring (Li *et al.*, 2007). In *C. albicans* $\Delta cho1$ cells, Sec3 localizes normally to the septum, showing that the inefficient

localisation of Exo84 in $\Delta cho1$ cells is specific and not due to general disorganisation of the polarity machinery. A possible role for the phosphorylation is that it promotes Exo84 recycling by lowering its affinity for PS. Its reduced rate of fluorescence recovery after photobleaching is consistent with this idea.

In conclusion, the special growth characteristics of *C. albicans* hyphae have revealed a previously hidden role for Exo84 phosphorylation by a cyclin-dependent kinase. Rather than causing cell surface expansion to cease during mitosis, phosphorylation is necessary for the efficient polarized growth of hyphae possibly by altering Exo84 affinity for PS in the cell membrane. The different actions on Exo84 of Cdk1-Hgc1 in *C. albicans* and Cdk1-Clb2 in *S. cerevisiae* are consistent with the different patterns of the Cdk1 target sites in the two proteins. *CaExo84* contains a Cdk1 phosphorylation site in the PH domain explaining the reduction in its affinity for PS, while *ScExo84* contains a phosphorylation site in the C-terminal interaction domain explaining the loss of interaction with other exocyst subunits. Thus, while *EXO84* is present in the genomes of both species, it has evolved so that its phosphorylation adapts each organism to its particular pattern of growth.

Materials and Methods

Media and growth conditions

YEPD consists of 2% glucose, 2% Difco Bacto peptone and 1% Difco Bacto yeast extract plus 80 mg.l⁻¹ uridine. SD medium consists of 0.67% w/v yeast nitrogen base (Difco), 2% w/v glucose, 80 mg.l⁻¹ each of uridine or 40 mg.l⁻¹ histidine, and arginine. Hyphae were induced from unbudded stationary phase yeast cells as described previously. The $\Delta cho1$ mutant was grown in synthetic defined (SD) medium containing 1 mM ethanolamine and hyphal growth was induced in Lee's medium (Lee *et al.*, 1975). Shutdown of *pMET3-CLB2* experiments were carried out in SD supplemented with 10 mM methionine and 2.5 mM cysteine.

Strains and plasmids constructions

Strains constructed are listed in Table S1, and the oligonucleotides used are listed in Table S2. All strains were derived from BWP17 (Wilson *et al.*, 1999). Gene deletions and C-terminal YFP fusions and HA fusions were performed as previously described (Gola *et al.*, 2003; Lavoie *et al.*, 2008; Schaub *et al.*, 2006; Walther and Wendland, 2007). All strains were checked for correct genome integration by PCR. Correct expression of protein fusion strains were also verified by Western blot using antibodies to the fusion protein or epitope (data not shown).

Generation of *EXO84* mutant alleles was carried out as described previously (Court and Sudbery, 2007).

Western blots

Western blots were carried out as described previously (Wightman *et al.*, 2004).

2D gel electrophoresis

Exo84-YFP was immunoprecipitated as previously described and then eluted from beads with hydration buffer (8 mM urea, 2 M thiourea, 4% 3-[(3-cholamidopropyl)dimethylammonio]-1-propanesulfonate (CHAPS), 1 mM dithiothreitol (DTT), 0.5% IPG buffer pH 3-10, and 1.2% DeStreak Reagent) (GE Healthcare). The immunoprecipitated protein was resolved on 2D gels using 7-cm Immobiline DryStrip pH 3-10 and the Ettan IPGphor 3 Isoelectric Focusing System (GE Healthcare).

Exocyst complex Co-Immunoprecipitation

Cells were broken in IP-Lysis buffer (5% glycerol, 50 mM TRIS-HCl pH 7.5, 150 mM KCl, 2 mM MgCl₂, 0.5 mM EGTA, 1 mM DTT, and protease inhibitors tablet (Roche)). Immunoprecipitation was made as described above using anti-GFP or anti-HA antibodies

In vitro kinase assays

Cdc28-HA or Cdc28as-HFP was immunoprecipitated from hyphal lysates using anti-HA (12CA5, monoclonal antibody). Kinase assays were carried out as previously described (Bishop et al., 2010). The α pS-Cdk antibody was used to detect Cdk1-specific phosphorylation.

Phospholipid-binding assay.

Recombinant GST-Exo84, GST-Exo84-3A, and GST-Exo84-3E were expressed in *E. coli* and purified with glutathione sepharose 4b (GE Healthcare) according to the manufacturer's instructions. For the strips shown in Fig. 9C 8 μ g of purified GST-Exo84-3E and 2 μ g of purified GST-Exo84 protein were incubated with PIP Strip (Echelon Biosciences, Salt Lake City, UT, USA) previously blocked with 3% BSA. Protein binding was visualized using anti-GST antibody (Santa Cruz Biotechnology Dallas, USA).

Microscopy

Live cell imaging was carried out on cells growing on agar pads using a Delta Vision RT microscope (Applied Precision Instruments, Seattle) as described previously (Bishop et al., 2010). The intensity of the Mlc1-YFP signal in the Spitzenkörper shown in Fig. 2 was measured using the plot Z axis profile tool in the FIJI distribution of NIH ImageJ (<http://fiji.sc/Fiji>) after a ROI had been drawn around the area occupied by the Spitzenkörper in frames 43-58 of movie 2. The data are shown with the background measured within the cell subtracted. The images shown in Fig. 5 were obtained from cells which were grown in YEPD liquid culture 120 mins after hyphal induction and stained in PBS buffer with Calcofluor white (Fluorescent Brightener 28, Sigma Aldrich) at a concentration of 1 μ g.ml⁻¹. To quantify cell dimensions and morphology shown in Fig. 5 hyphal cells were grown for 120 minutes in YEPD liquid culture as described above. After harvesting the cells were fixed with 2% formaldehyde and then treated with pepsin to dissociate clumped hyphae as previously described (Sudbery, 2001). Cell dimensions were measured using FIJI aided by an in-house custom script that recorded cell dimensions and user-defined definitions of morphological state (hyphae, pseudohyphae or other). Calcofluor white (Fluorescent Brightener 28, Sigma Aldrich) was added to liquid grown cells at a concentration of 1 μ g.ml⁻¹. FRAP experiments were carried out using the Delta Vision Microscope with an attached 532 nm laser module used for bleaching. Images were analysed in FIJI as follows. For each image a threshold set to exclude the background. An ROI was drawn around the crescent of Exo84 in the pre-bleach image. The fractional area above the threshold in pre-bleach, post-bleach and post bleach plus 30s images was then recorded. Recovery was defined as $(I_{30}-I_b)/(I_0-I_b) \times 100\%$ where I_0 , I_b , I_{30} are the values of Exo84-YFP intensity pre-bleach, post-bleach and 30s post bleach respectively

Protein threading

The Protein Homology/Analogy Recognition Engine V2.0 (Phyre2) in its intensive modelling mode was used to obtain Exo84 structure (Kelley and Sternberg, 2009). Analysis, formatted and final movies and images were created using PyMOL (PyMOL Molecular Graphics System, Version 1.2r3pre, Schrödinger, LLC.)

Acknowledgements

We thank Jeremy Craven and Sam Barnett for custom scripts to run within the FIJI version of ImageJ that was used in the quantitation of the micrographs. We thank the Berman, Wang and Wendland laboratories for strains and plasmids. This work was supported by BBSRC project grant BB/J002305/1.

Authorship Contributions

D.C-L conceived and designed the study with input from P.E.S. D.C-L performed all the experiments except the live cell movies which were carried out by P.E.S. P.E.S and D.C-L interpreted the data. P.E.S wrote the manuscript with input from D.C-L.

The authors declare they have no conflict of interest

Reference List

- Adamo, J.E., Rossi, G., and Brennwald, P. (1999). The Rho GTPase Rho3 has a direct role in exocytosis that is distinct from its role in actin polarity. *Mol Biol Cell* 10, 4121-4133.
- Bensen, E.S., Clemente-Blanco, A., Finley, K.R., Correa-Bordes, J., and Berman, J. (2005). The mitotic cyclins Clb2p and Clb4p affect morphogenesis in *Candida albicans*. *Mol Biol Cell* 16, 3387-3400.
- Bishop, A., Lane, R., Beniston, R., Lazo, B., Smythe, C., and Sudbery, P. (2010). Hyphal growth in *Candida albicans* requires the phosphorylation of Sec2 by the Cdc28-Ccn1/Hgc1 kinase. *EMBO J* 29, 2930-2942.
- Boyd, C., Hughes, T., Pypaert, M., and Novick, P. (2004). Vesicles carry most exocyst subunits to exocytic sites marked by the remaining two subunits, Sec3p and Exo70p. *J Cell Biol* 167, 889-901.
- Brennwald, P. and Rossi, G. (2007). Spatial regulation of exocytosis and cell polarity: Yeast as a model for animal cells. *FEBS Letters* 581, 2119-2124.
- Caballero-Lima, D., Kaneva, I.N., Watton, S.P., Sudbery, P.E., and Craven, C.J. (2013). The Spatial Distribution of the Exocyst and Actin Cortical Patches Is Sufficient To Organize Hyphal Tip Growth. *Euk Cell* 12, 998-1008.
- Chapa Y Lazo, B., Lee, S., Regan, H., and Sudbery, P. (2011). The mating projections of *Saccharomyces cerevisiae* and *Candida albicans* show key characteristics of hyphal growth. *Fungal Biology* 115, 547-556.
- Chen, Y.L., Montedonico, A.E., Kauffman, S., Dunlap, J.R., Menn, F.M., and Reynolds, T.B. (2010). Phosphatidylserine synthase and phosphatidylserine decarboxylase are essential for cell wall integrity and virulence in *Candida albicans*. *Mol Microbiol* 75, 1112-1132.
- Court, H. and Sudbery, P. (2007). Regulation of Cdc42 GTPase activity in the formation of hyphae in *Candida albicans*. *Mol Biol Cell* 18, 265-281.
- Crampin, H., Finley, K., Gerami-Nejad, M., Court, H., Gale, C., Berman, J., and Sudbery, P.E. (2005). *Candida albicans* hyphae have a Spitzenkorper that is distinct from the polarisome found in yeast and pseudohyphae. *J Cell Sci* 118, 2935-2947.

- Finger, F.P., Hughes, T.E., and Novick, P. (1998). Sec3p is a spatial landmark for polarized secretion in budding yeast. *Cell* 92, 559-571.
- Gola, S., Martin, R., Walther, A., Dunkler, A., and Wendland, J. (2003). New modules for PCR-based gene targeting in *Candida albicans*: rapid and efficient gene targeting using 100 bp of flanking homology region. *Yeast* 20, 1339-1347.
- Goranov, A.I. and Amon, A. (2010). Growth and division not a one-way road. *Curr Opin Cell Biol* 22, 795-800.
- Guo, W., Tamanoi, F., and Novick, P. (2001). Spatial regulation of the exocyst complex by Rho1 GTPase. *Nat Cell Biol* 3, 353-360.
- He, B. and Guo, W. (2009). The exocyst complex in polarized exocytosis. *Curr Opin Cell Biol* 21, 537-542.
- He, B., Xi, F., Zhang, X., Zhang, J., and Guo, W. (2007a). Exo70 interacts with phospholipids and mediates the targeting of the exocyst to the plasma membrane. *EMBO J* 26, 4053-4065.
- He, B., Xi, F.G., Zhang, J., TerBush, D., Zhang, X.Y., and Guo, W. (2007b). Exo70p mediates the secretion of specific exocytic vesicles at early stages of the cell cycle for polarized cell growth. *J Cell Biol* 176, 771-777.
- Heider, M.R. and Munson, M. (2012). Exorcising the Exocyst Complex. *Traffic* 13, 898-907.
- Jones, L.A. and Sudbery, P.E. (2010). Spitzenkorper, exocyst and polarisome components in *Candida albicans* hyphae show different patterns of localization and have distinct dynamic properties. *Euk Cell* 9, 1455-1465.
- Kelley, L.A. and Sternberg, M.J. (2009). Protein structure prediction on the Web: a case study using the Phyre server. *Nature Protocols* 4, 363-371.
- Klis, F.M., Boorsma, A., and De Groot, P.W.J. (2006). Cell wall construction in *Saccharomyces cerevisiae*. *Yeast* 23, 185-202.
- Lavoie, H., Sellam, A., Askew, C., Nantel, A., and Whiteway, M. (2008). A toolbox for epitope-tagging and genome-wide location analysis in *Candida albicans*. *BMC Genomics* 9, 578-591.
- Lee, K.L., Buckley, H.R., and Cambell, C.C. (1975). An amino acid liquid synthetic medium for the development of mycelial and yeast forms of *Candida albicans*. *Sabouraudia* 13, 148-153.
- Li, C.R., Lee, R.T.-H., Wang, Y.M., Zheng, X.D., and Wang, Y. (2007). *Candida albicans* hyphal morphogenesis occurs in Sec3p-independent and Sec3p-dependent phases separated by septin ring formation. *J Cell Sci* 120, 1898-1907.
- Luo, G., Zhang, J., Luca, F.C., and Guo, W. (2013). Mitotic phosphorylation of Exo84 disrupts exocyst assembly and arrests cell growth. *J Cell Biol* 202, 97-111.
- Luo, J.Y., Vallen, E.A., Dravis, C., Tcheperegine, S.E., Drees, B., and Bi, E.F. (2004). Identification and functional analysis of the essential and regulatory light chains of the only type II myosin Myo1p in *Saccharomyces cerevisiae*. *J Cell Biol* 165, 843-855.

- McCusker,D., Denison,C., Anderson,S, Egelhofer,T.A., Yates,J.R., Gygi,S.P., and Kellogg,D.R. (2007). Cdk1 coordinates cell-surface growth with the cell cycle. *Nat Cell Biol* 9, 506-U45.
- Punta,M. *et al.* (2012). The Pfam protein families database. *Nucleic Acids Res* 40, D290-D301.
- Roumanie,O., Wu,H., Molk,J.N., Rossi,G, Bloom,K, and Brennwald,P. (2005). Rho GTPase regulation of exocytosis in yeast is independent of GTP hydrolysis and polarization of the exocyst complex. *J Cell Biol* 170, 583-594.
- Sandquist,J.C., Kita,A.M., and Bement,W.M. (2011). And the Dead Shall Rise: Actin and Myosin Return to the Spindle. *Developmental Cell* 21, 410-419.
- Schaub,Y., Dunkler,A., Walther,A., and Wendland,J (2006). New pFA-cassettes for PCR-based gene manipulation in *Candida albicans*. *Journal of Basic Microbiology* 46, 416-429.
- Snha,I., Wang,Y.M., Philp,R, Li,C.R., Yap,W.H., and Wang,Y. (2007). Cydin-dependent kinases control septin phosphorylation in *Candida albicans* hyphal development. *Developmental Cell* 13, 421-432.
- Sniosoglou,S and Pelham,H.R.B. (2002). Vps51p links the VFT complex to the SNARE Tlg1p. *J. Biol. Chem.* 277, 48318-48324.
- Soll,D.R, Herman,M.A., and Staebell,M.A. (1985). The involvement of cell wall expansion in the two modes of mycelium formation of *Candida albicans* *JGen Microbiol* 131, 2367-2375.
- Sudbery,P.E (2001). The germ tubes of *Candida albicans* hyphae and pseudohyphae show different patterns of septin ring localisation. *Mol Microbiol* 41, 19-31.
- Sudbery,P.E (2011). Growth of *Candida albicans* hyphae. *Nat Rev Microbiol* 9, 737-748.
- Sudbery,P.E, Gow,N.A.R, and Berman,J (2004). The distinct morphogenic states of *Candida albicans*. *Trends Microbiol* 12, 317-324.
- Terbush,D.R., Maurice,T., Roth,D., and Novick,P. (1996). The exocyst is a multi-protein complex required for exocytosis in *Saccharomyces cerevisiae*. *EMBO J* 15, 6483-6494.
- Terbush,D.R and Novick,P. (1995). Sec6, Sec8, and Sec15 are components of a multisubunit complex which localizes to small bud tips in *Saccharomyces cerevisiae*. *J Cell Biol* 130, 299-312.
- Walther,A. and Wendland,J (2007). Hyphal Growth and Virulence. In: *Hyphal growth and Virulence*, ed. A.BrakhageBerlin, Heidelberg, New York: Springer-Verlag.
- Wang,A., Raniga,P.P., Lane,S, Lu,Y., and Liu,H.P. (2009). Hyphal Chain Formation in *Candida albicans*: Cdc28-Hgc1 Phosphorylation of Efg1 Represses Cell Separation Genes. *Mol Cell Biol* 29, 4406-4416.
- Wightman,R, Bates,S, Amnorrattapan,P., and Sudbery,P.E (2004). In *Candida albicans*, the Nim1 kinases Gin4 and Hsl1 negatively regulate pseudohypha formation and Gin4 also controls septin organization. *JCell Biol* 164, 581-591.
- Wilson,B, Davis,D., and Mitchell,A.P. (1999). Rapid hypothesis testing in *Candida albicans* through gene disruption with short homology regions. *JBacteriol* 181, 1868-1874.

Wu,H., Turner,C., Gardner,J., Temple,B., and Brennwald,P. (2010). The Exo70 Subunit of the Exocyst Is an Effector for Both Cdc42 and Rho3 Function in Polarized Exocytosis. *Mol Biol Cell* 21, 430-442.

Zhang,X, Orlando,K, He,B, Xi,F, Zhang,J, Zajac,A., and Guo,W. (2008). Membrane association and functional regulation of Sec3 by phospholipids and Cdc42. *JCell Biol* 180, 145-158.

Zhang,X.Y., Bi,E.F., Novick,P., Du,LL, Kozminski,K.G., Lipschutz,J.H., and Guo,W. (2001). Cdc42 interacts with the exocyst and regulates polarized secretion. *JBiol Chem* 276, 46745-46750.

Zheng,X, Wang,Y., and Wang,Y. (2004). Hgc1, a novel hypha-specific G1 cyclin-related protein regulates *Candida albicans* hyphal morphogenesis. *EMBO J*23, 1845-1856.

Zheng,X.D., Lee,R.T.H., Wang,Y.M., Lin,Q.S, and Wang,Y. (2007). Phosphorylation of Rga2, a Cdc42 GAP, by CDK/Hgc1 is crucial for *Candida albicans* hyphal growth. *EMBO J*26, 3760-3769.

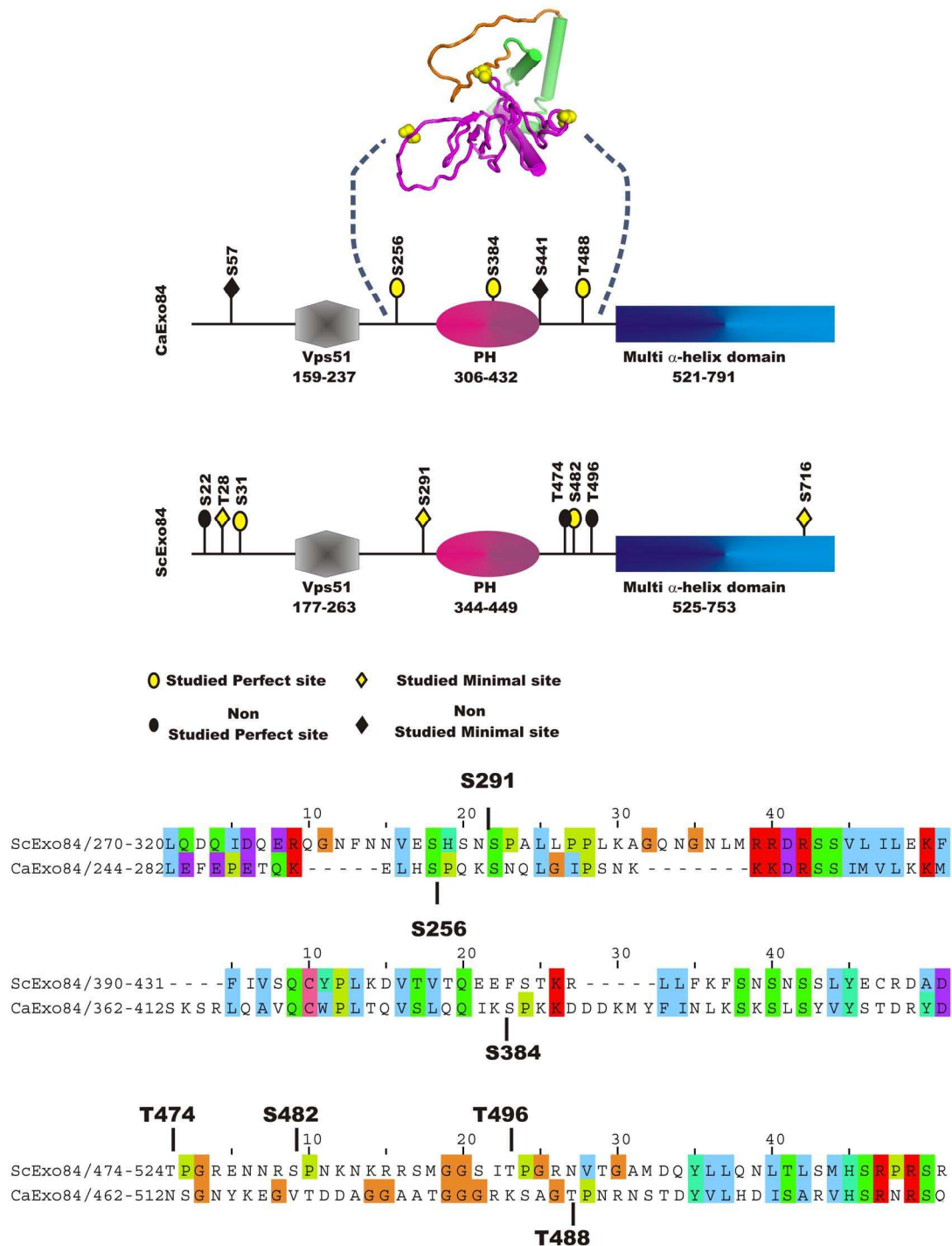


Fig. 1. Domain organisation and Cdk1 target sites of ScExo84 and CaExo84. A: Domain organisation and Cdk1 target sites. The VPS51 domain was identified in both CaExo84 and ScExo84 using the Pfam database (Punta *et al.*, 2012). The PH domain and the C-terminal interaction domain was identified by threading as described in materials and methods. Studied sites refers to this paper for CaExo84 and Luo *et al.* (Luo *et al.*, 2004) for ScExo84. The folding structure of the PH domain predicted by threading is shown in purple. Phosphorylation of potential Cdk1 target sites is shown by the yellow spheres. S284 lies within a protruding loop of the PH domain and S256 and T488 are located at the boundaries of the PH domain. B: Clustal alignments of sequences surrounding full Cdk1 sites in CaExo84. Colour code follows standard Clustal X code: amino acids with similar properties are coded with the same colour; the depth of the colour denotes the degree of similarity, so that identical residues have the deepest colour.

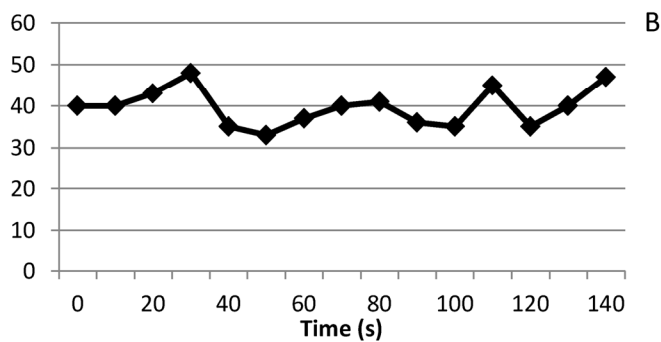
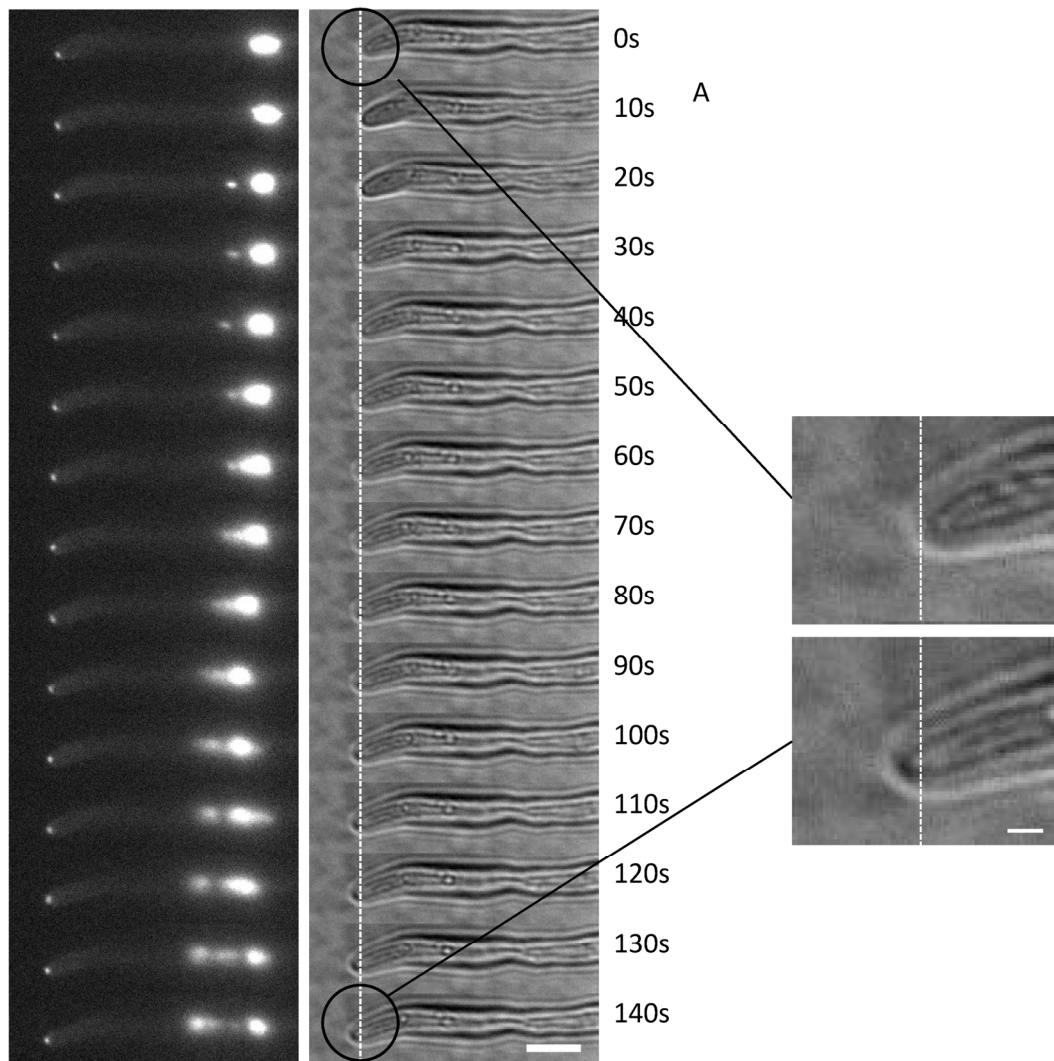


Fig. 2 Growth does not stop during mitosis. A: Single frames from Nop1-YFP Mlc1-YFP undergoing mitosis. Images were recorded at 10s intervals. In order to reduce phototoxicity and photobleaching a single Z-plane was recorded at each time point using 50ms exposure. The full movie is shown in movie 2. Shown here is a montage, generated using the FIJI version of ImageJ, which shows successive images with the initial image starting at frame 43 of the full movie. Left column: fluorescent images showing Mlc1-YFP at the hyphal tip and the Nop1-YFP in the nucleus. The satellite spot may represent Mlc1 in the Spindle pole body. Right column DIC images for corresponding fluorescent images in the left column. The dash line is a vertical line dropped from the hyphal tip in the 0s frame which reveals the continual extension of the hyphal tip throughout the image series. The hyphal tip in the initial and final frames is enlarged to show that throughout the

140s of image series the tip extends by approximately $0.8 \mu\text{m}$ consistent with the $0.33 \mu\text{m min}^{-1}$ long term average rate of hyphal growth (Figs S1 and Movie 1). Scale bar in the main image series = $5\mu\text{m}$; scale bar in the enlargement = $1\mu\text{m}$. B: The maximum intensity of the Mlc1 spot in the image series was measured using ImageJ, the background subtracted and plotted against time. Units on the ordinate are arbitrary units.

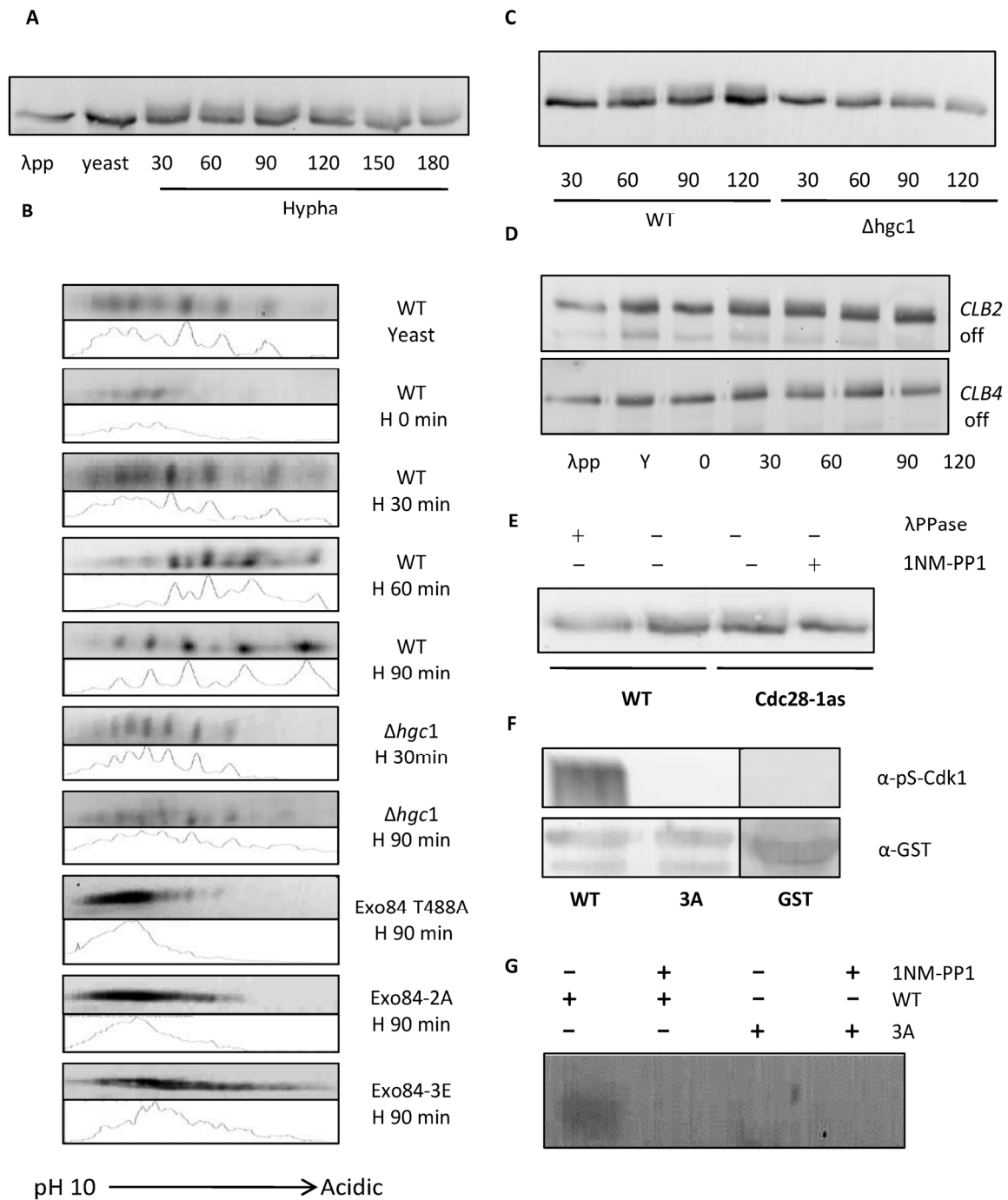


Fig. 3 Exo84 is phosphorylated by Cdk1. **A:** Western blot using anti-GFP antisera of Exo84-YFP from yeast and hyphae as indicated. Numbers below hypha indicate time in minutes since unbudded stationary phase cells were induced to form hyphae. λPP: Lambda phosphatase treated sample. **B:** 2D gels of Exo84-YFP from lysates of wild type (WT) and $\Delta hgc1$ strains from WT unbudded stationary phase cells (WT H 0 mins) and from hyphae induced from WT cells after 30, 60 and 90 minutes and $\Delta hgc1$ after 30 and 90 minutes as indicated. The stationary phase cells were also reinoculated into yeast growth medium and lysates prepared after 3 hours when the cells were in exponential growth (WT Yeast). **C:** Exo84 extracted from $\Delta hgc1$ cells is less phosphorylated shown by the absence of the slower migrating smear present in Exo84 extracted from wild type cells. **D:** Exo84 is still phosphorylated in cells depleted of Clb2 and Clb4. **E:** Phosphorylation of Exo84 is inhibited by 1NM-PP1 when the strain carries the $cdk1-1as$ allele **F:** Recombinant GST-Exo84 but not recombinant GST-

Exo84-3A is phosphorylated *in vitro* by Cdk1. The indicated recombinant forms of GST-Exo-84 or GST alone were incubated in kinase reaction buffer with immunoprecipitated Cdk1-HA. The product were analysed on a Western blot using the α S-Cdk1 antibody. G: The *in vitro* kinase reaction is inhibited by 1NM PP1 when the purified kinase carries the analog-sensitive cdk1-1as allele.

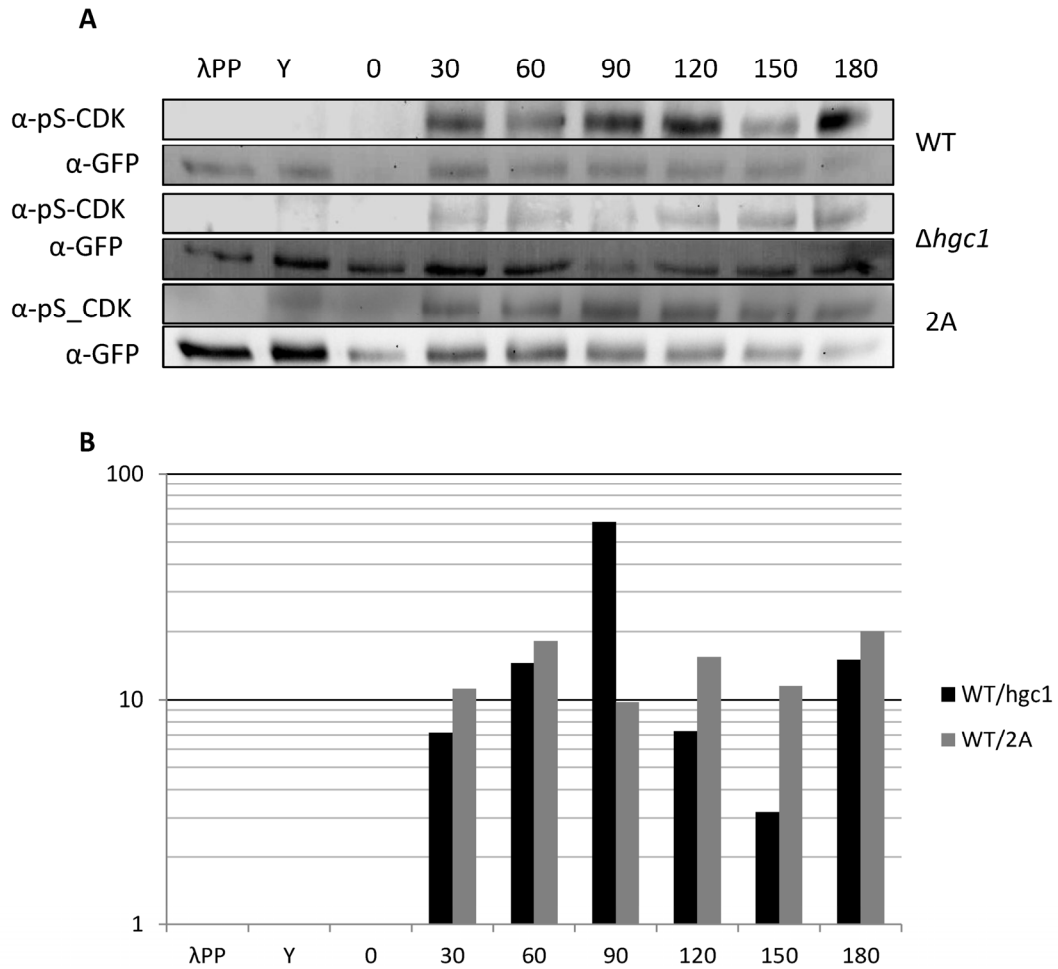


Fig. 4 Phosphorylation of Exo84-YFP detected by the α pS-Cdk1 antibody is reduced in Exo84-2A or in cells lacking Hgc1. Membranes were stripped and reprobbed with an anti-GFP antibody as a loading control. B: Ratios of the wild type to mutant intensities of the α pS-Cdk1 signals normalised by the GFP loading controls.

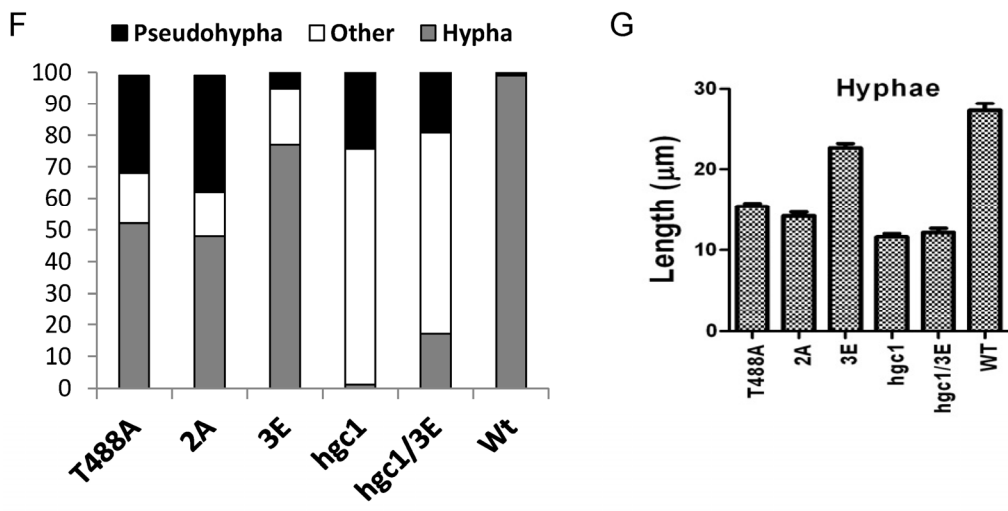
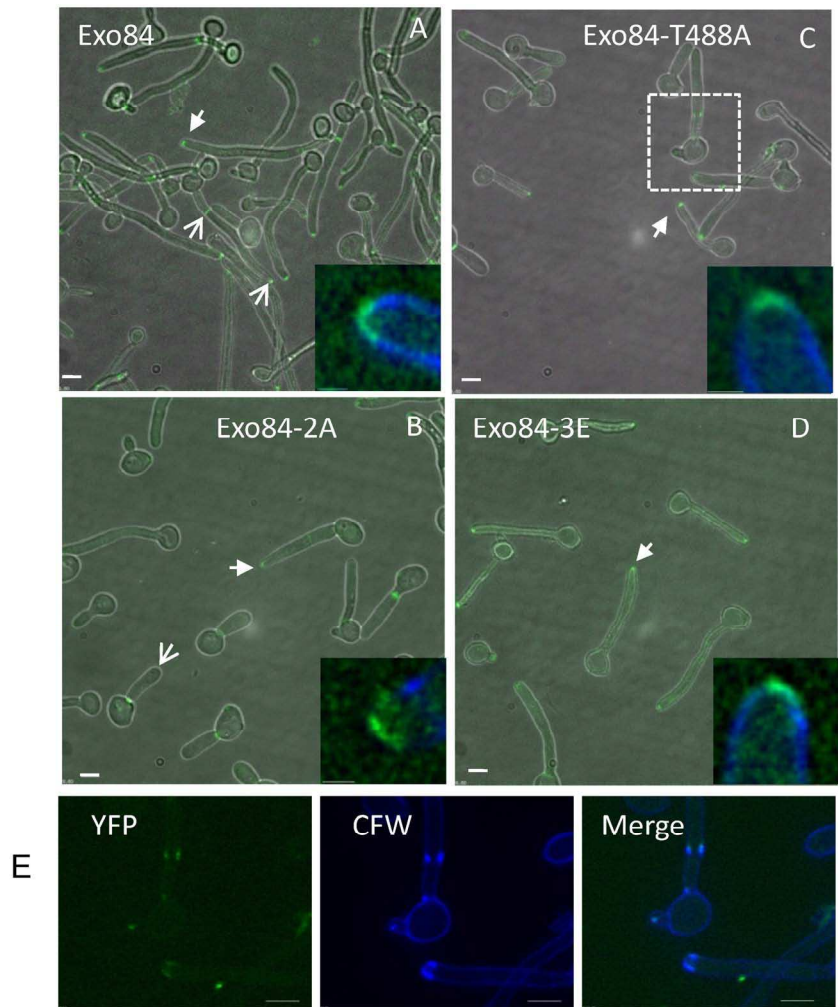


Fig. 5 Phenotype of cells expressing non-phosphorylatable or phosphomimetic substitutions. A-D: Appearance cells expressing the indicated proteins fused to YFP 120 minutes after hyphae were induced from unbudded stationary phase yeast cells. Cells were harvested and resuspended in PBS containing Calcofluor white (CFW). The main images show the merged YFP-DIC channels. Insets show enlargements of the merged YFP and blue CFW channels of the tips indicated by solid arrows. (Pixilation in the inset images was smoothed with Softworx interpolated zoom function). Panel A barbed arrows indicate a hypha where YFP is simultaneously present at the tip and septum. Panel B

barbed arrow indicates a pseudohypha with YFP at the septum but not the tip. Scale bars: Main image 5 μ m; insets 1 μ m. E: Enlargement of the YFP, CFW and merged images in the area bounded by dashed lines in panel C. Scale bars 5 μ m. F: quantitation of morphology of the indicated strains 120 minutes after hyphal induction was carried out based on criteria described previously (Sudbery *et al.*, 2004). Cells were classified as hyphae where the daughter compartment was narrow (< 2 μ m), had parallel sides, and where CFW staining (not shown) showed first septum was within the germ tube. Cells were classified as pseudohyphae when the width was greater than 2 μ m, there was a constriction and a septum at the neck of mother cell-daughter compartment, and the sides were not parallel. Cells were classified as "other" when a short parallel-sided germ tube swelled to form a less polarised compartment. A minimum of 150 cells were classified for each strain. G: In the same cells the length of the hyphal compartment was measured.

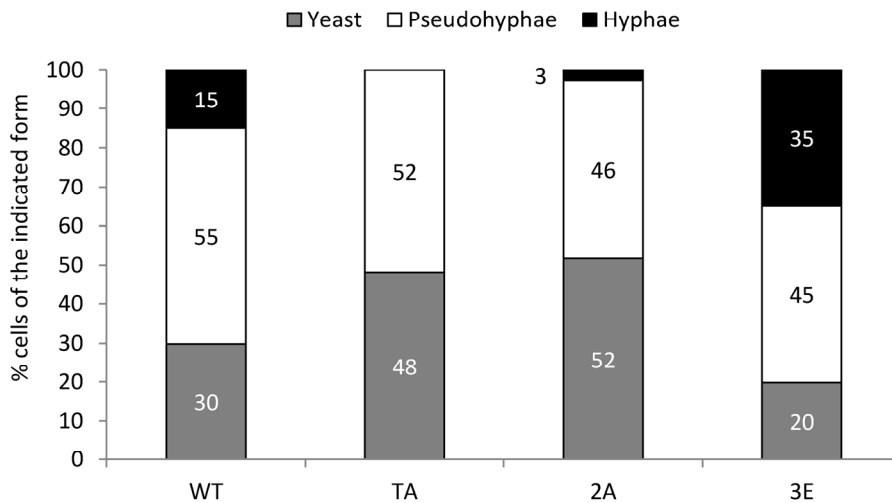
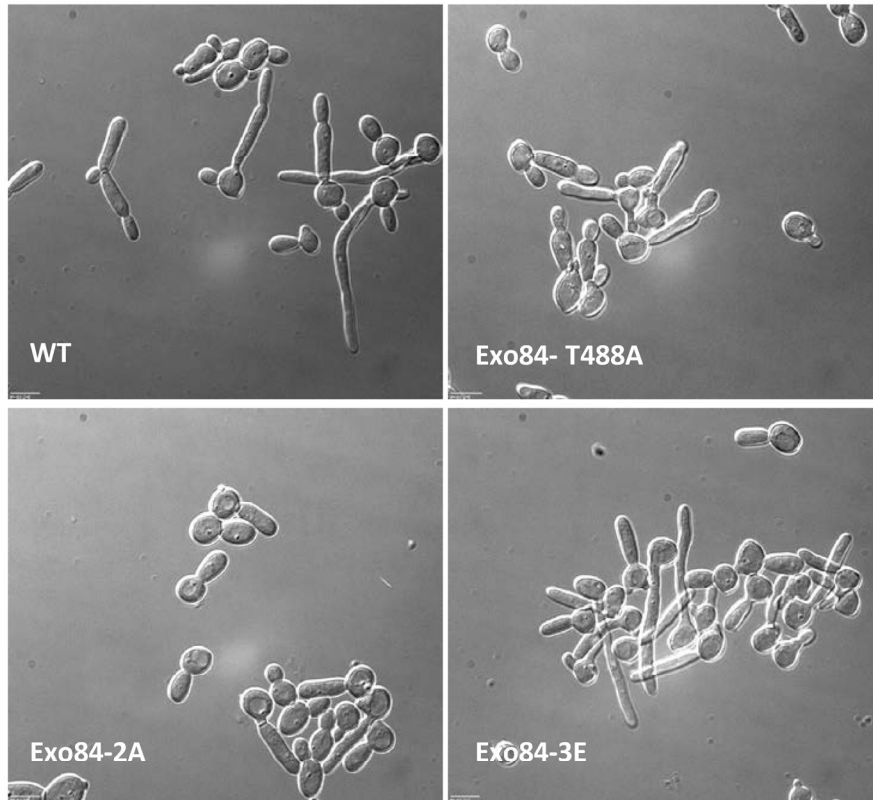


Fig. 6. The phosphomimetic *EXO84-3E* allele promotes hyphal growth under pseudohyphal growth conditions. Stationary phase cells were inoculated into YEPD pH 6.0 and cultured at 35°C. Morphology was classified as described in the legend for Fig. 5. A minimum of 150 cells were classified for each strain.

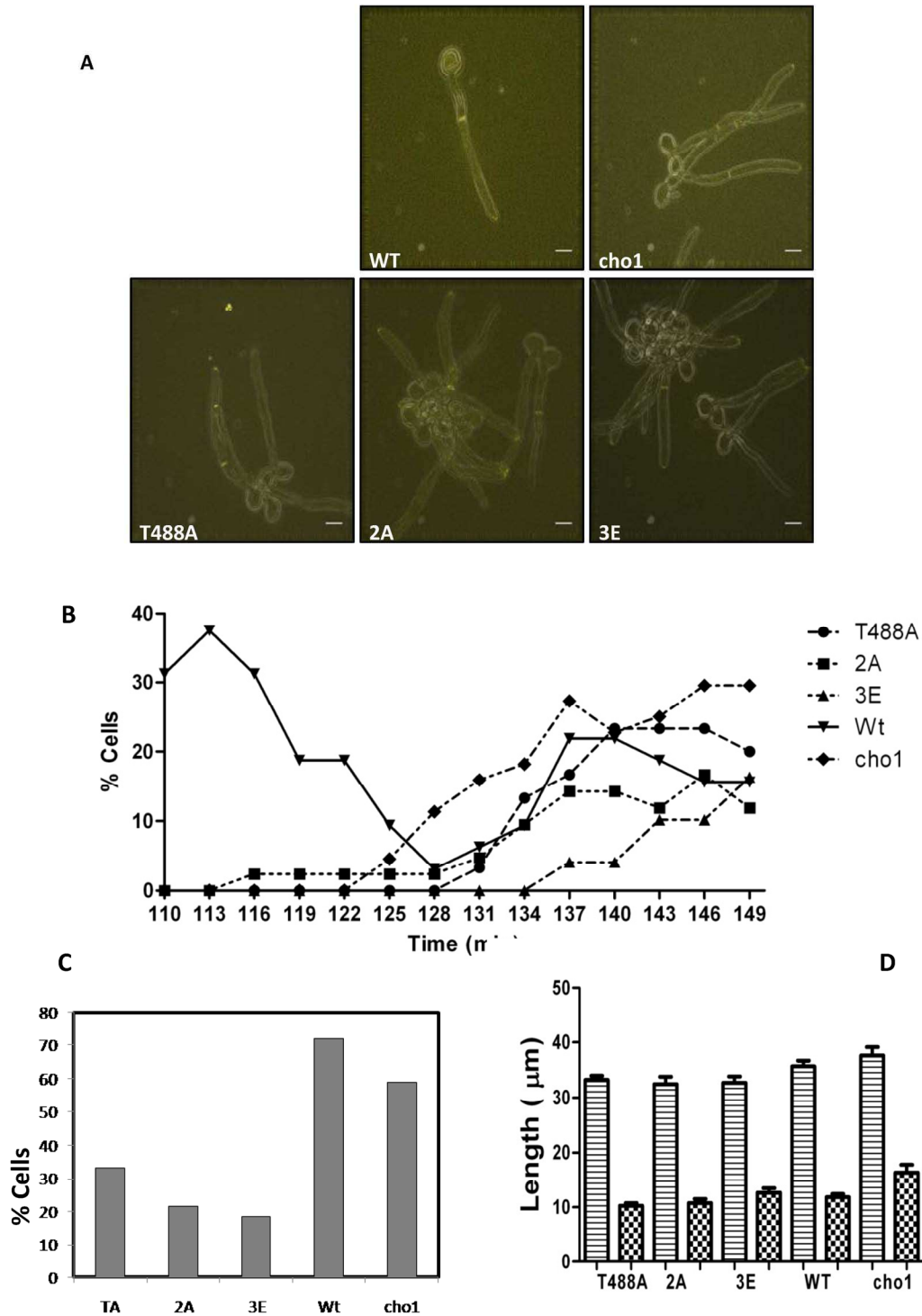


Fig. 7 Effect of Exo84 phospho-acceptor site mutations on the localization of Exo84-YFP in hyphal cells. Individual cells of the indicated strains were grown on agar pads containing minimal medium as described previously (Bishop *et al.*, 2010) and at 3 minute intervals each cell was examined to determine if Exo84-YFP had located to the septum. **A:** Appearance of cells where Exo84 is present at the tip and septum. The image is a merge image of the YFP fluorescence and the DIC images where the contrast of the DIC image has been increased to generate a cell outline. **B:** The percentage of cells showing Exo84 at the septum is plotted against time after hyphal induction. At least 10 cells were examined simultaneously for each strain. **C:** The cumulative total of cells where Exo84 had appeared at the septum after 150 minutes **D:** The length of the hypha when Exo84 first appeared at

the septum for each strain (horizontal hatch) and the distance of the septum from the bud neck (hatched bars) were recorded. Note the relevance of the $\Delta cho1$ mutant is described in the section "Phosphorylation of Exo84 may affect phospholipid binding"

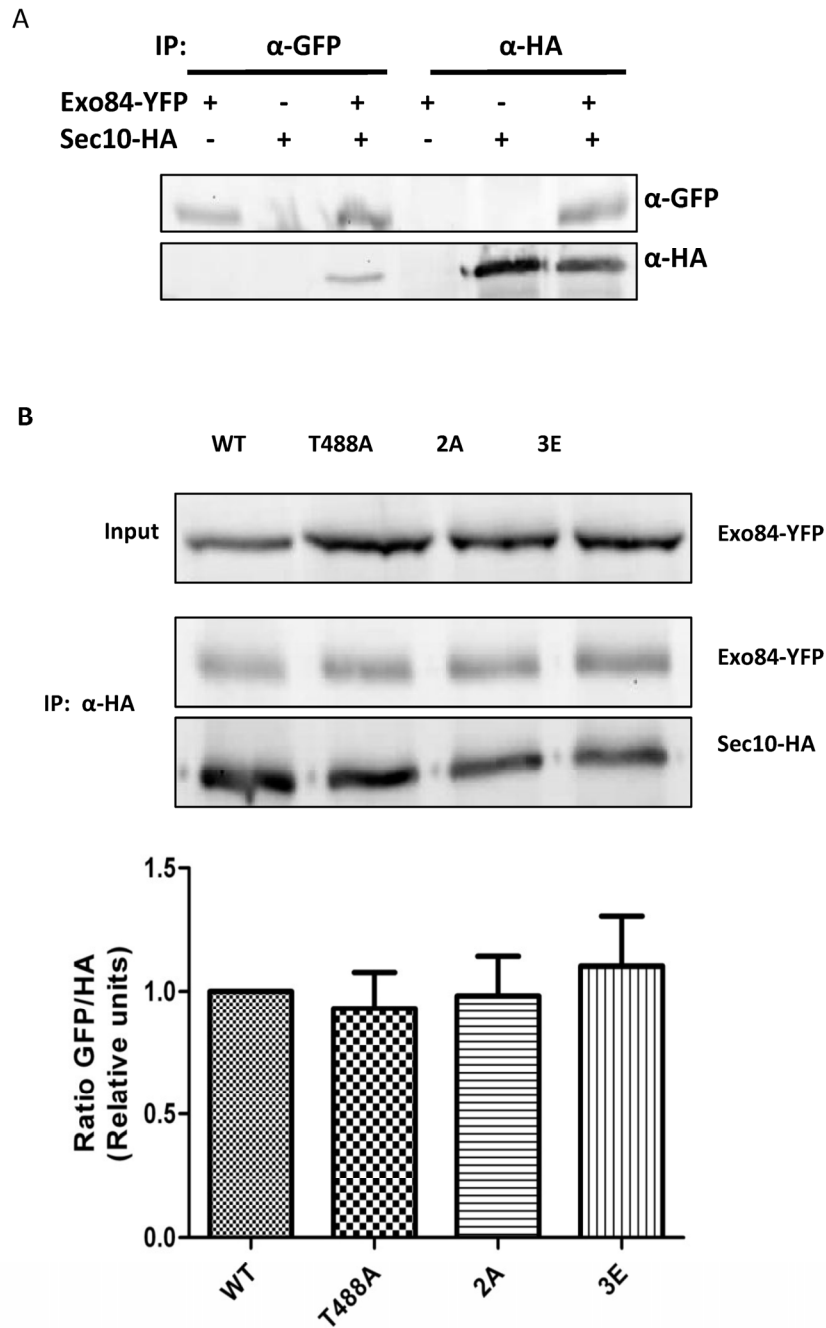


Fig. 8 Exo84 phospho site mutations do not disrupt the association with Sec10. a) Reciprocal Immunoprecipitation of Exo84-YFP with Sec10-HA. b) Immunoprecipitation of Sec10-HA with Exo84-YFP carrying the indicated mutations. Panel a) provides controls showing that the α GFP and α HA antibodies do not show non-specifically interactions.

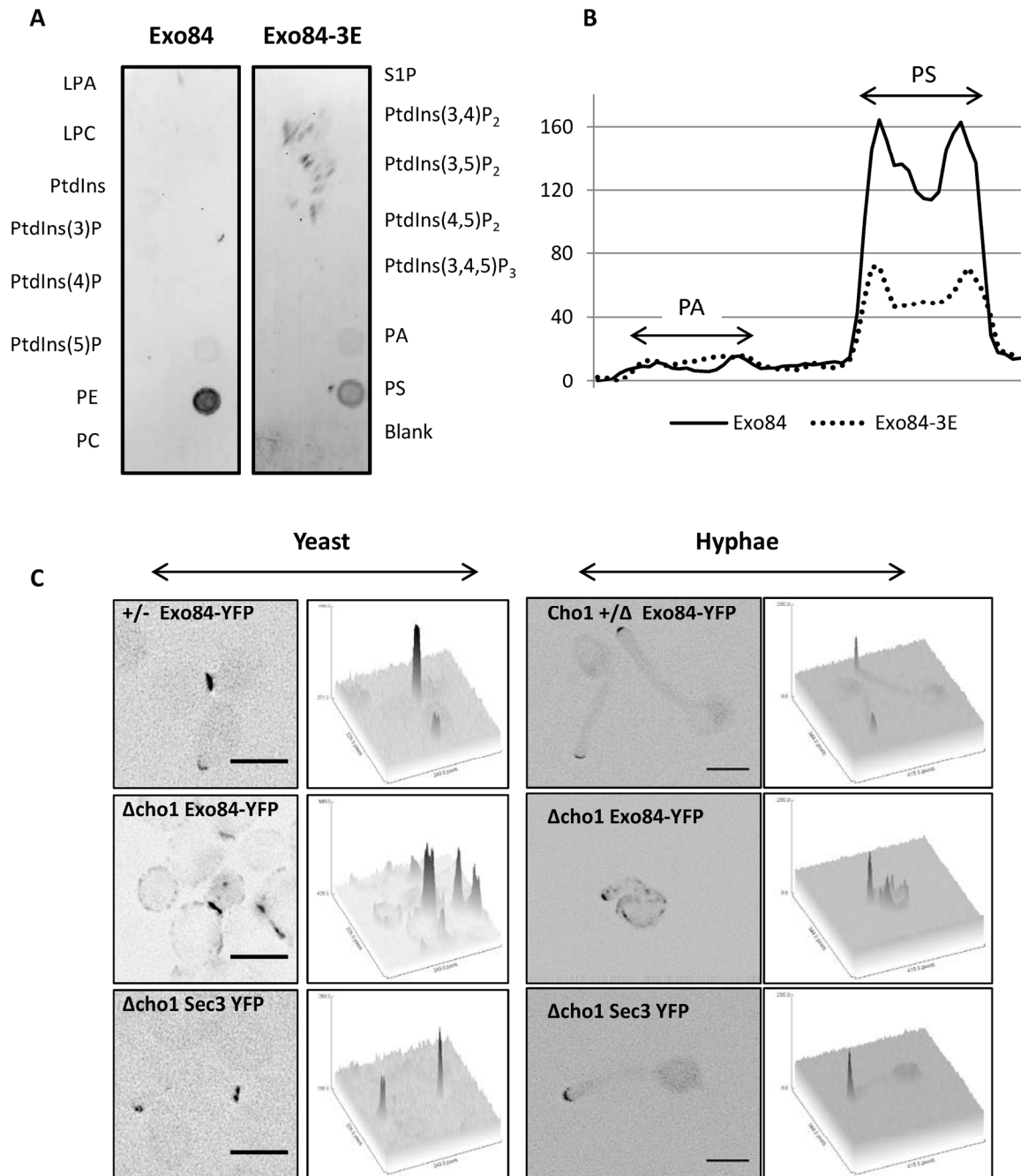


Fig. 9 Exo84 interacts with phosphatidylserine A: Binding of Exo84 to phospholipids. 2 μ g Recombinant GST-Exo84, and 8 μ g of GST-Exo84-3E were incubated with the phospholipid test strip. The phospholipids on the PIP strip are organised in two columns. The left column is labelled to the left of the Exo84 strip and the right column is labelled to the right of the Exo84-3E strip. PtdIns = phosphoinositol. PE = phosphatidylethanolamine. PS = phosphatidylserine PA = Phosphatidic acid. PC = Phosphatidylcholine, SIP = Sphingosine-1-phosphate, LPA = Lysophosphatidic acid, LPC = lysophosphocholine B: Profile Exo84 and Exo84-3E binding to PA and PS on PIP strip with the background subtracted. Units on the ordinate are arbitrary units. C: Exo84-YFP and Sec3-YFP distribution in heterozygous *CHO1*/ Δ *cho1* and Δ *cho1* yeast and hyphal cells as indicated. 3D quantitation of fluorescence intensity is presented alongside each fluorescence image which has been colour inverted for clarity.

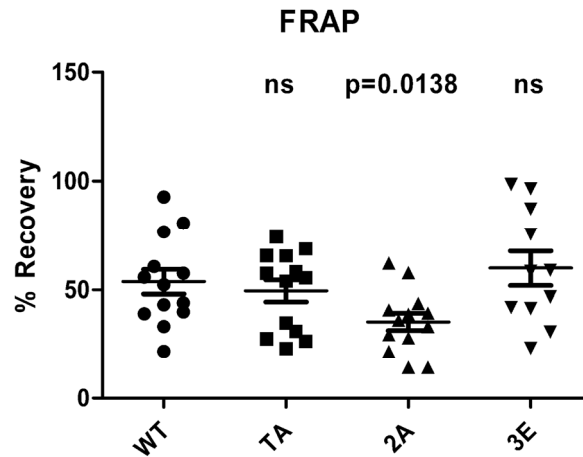


Fig. 10 Non-phosphorylatable substitutions reduce Exo84-YFP recovery after photobleaching. The indicated strains were grown as hyphae on agar pads in a DeltaVision microscope (TA = Exo84-EXO84 T488A). The tips were bleached using a laser. Images were recorded pre-bleach, post-bleach and post-bleach plus 30s. Exo84-YFP fluorescence was quantified as the fractional area of the tip above background fluorescence intensity. Recovery was defined as $(I_{30}-I_b)/(I_0-I_b) \times 100\%$; where I_0 , I_b , I_{30} are the values of Exo84-YFP fluorescence pre-bleach, post-bleach and 30s post bleach respectively. ns = non-significant ($p > 0.05$)